Mendeleev Communications

Mendeleev Commun., 2025, **35**, 583–585

Triblock P(D,L)LA-PEG-P(D,L)LA copolymer hydrogels with a variable ratio of hydrophilic and hydrophobic blocks

Yuliya S. Fomina,*[a] Yury D. Zagoskin,[a] Petr V. Dmitryakov,[a] Artem V. Bakirov,[a,b] Sergey N. Chvalun[a,b] and Timofey E. Grigoriev[a]

[a] *National Research Centre 'Kurchatov Institute', 123182 Moscow, Russian Federation. E-mail: fomina.uylia@yandex.ru*

[b] *N. S. Enikolopov Institute of Synthetic Polymeric Materials, Russian Academy of Sciences, 117393 Moscow, Russian Federation*

DOI: 10.71267/mencom.7768

A series of novel hydrogels were prepared *via* the solvent replacement method, employing triblock copolymers of D,L-lactide and ethylene glycol. These hydrogels demonstrated a prominent capacity to maintain and preserve their structural integrity; the resulting hydrogel materials exhibited a high elastic modulus, ranging from 7 ± 1 to 37 ± 4 kPa, depending on their composition. The network of hard blocks in these hydrogels was found to be well ordered, revealing a long period, detected by small angle X-ray scattering (SAXS); the order parameter value depends on polylactide chain length.

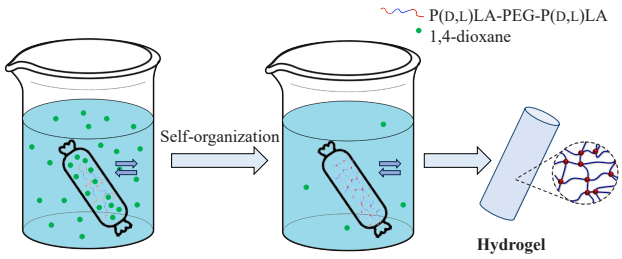

Keywords: hydrogel, amphiphilic block copolymer, SAXS, polylactide, polyethylene glycol.

Hydrogel colloidal systems contain a three-dimensional network of polymer clusters in water. Biocompatible and biodegradable hydrogels are very promising for biomedical applications in tissue engineering[1–3] and targeted drug delivery[4] due to their high water content and tunable modification of their physical and mechanical properties.

In this work, triblock copolymers of lactide and ethylene glycol (PLA-PEG-PLA) were chosen due to their high potential as a polymer matrix.[3,5,6] Such systems are capable of forming physically cross-linked hydrogels.[7–11]

It is known that aqueous solutions of similar block copolymers exhibit a sol–gel–sol phase transition within a specific temperature and concentration range. Each of these transitions is characterized by a gelation temperature.[7–11] Such behavior could be relevant for the creation of injection systems for minimally invasive medical treatments. A notable disadvantage associated with these materials is that they exhibit poor mechanical characteristics in comparison with covalently cross-linked systems because of the weaker interactions that stabilize the polymer matrix. In a substantial number of publications, the storage moduli G' for hydrogels based on PLA-PEG-PLA block copolymers with amorphous hydrophobic blocks do not exceed 1–10 kPa, and they are often incapable of holding their shape.[7–11] The lack of advanced techniques for the fabrication of PLA-PEG-PLA-based hydrogels with control of their physical and mechanical properties only underlines the significance of the presented investigation.

The objective of the research was to develop a method for the preparation of hydrogel systems based on copolymers of lactide and ethylene glycol with amorphous hydrophobic blocks, characterized by high elasticity, and to determine the influence of the composition of the high-molecular compound on the structure and mechanical characteristics of the resulting hydrogels.

In the present work, a series of triblock P(D,L)LA-PEG-P(D,L)LA copolymers was synthesized (Scheme 1) by ring-opening polymerization[3,5–8,12] of D,L-lactide initiated by PEG (see details in Online Supplementary Materials).

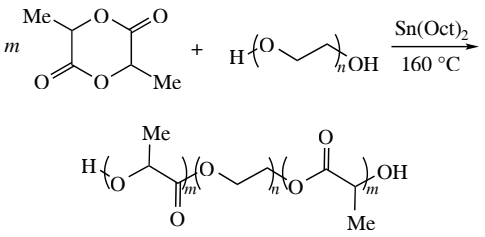

Scheme 1 Synthesis of triblock P(D,L)LA-PEG-P(D,L)LA copolymers. $Sn(Oct)_2$ is tin(II) 2-ethylhexanoate.

The molecular weight characteristics of the obtained block copolymers determined by gel permeation chromatography (number-average molecular weight M_n^a and polydispersity index M_w^a/M_n^a, see Figure S1, Online Supplementary Materials) and ^{1}H NMR spectroscopy (degree of polymerization of PLA-blocks (D,L), M_n^b and monomer conversion, see Figure S2, Online Supplementary Materials) are presented in Table 1.

Table 1 Molecular weight characteristics of block copolymers.

Sample	M_n^a/kDa	M_w^a/M_n^a	M_n^b/kDa	Conversion (%)
P_{136}	6.5	1.1	–	–
$DL_{41}P_{136}DL_{41}$	10.4	1.2	11.9	96.0
$DL_{72}P_{136}DL_{72}$	15.7	1.2	16.4	95.0
$DL_{101}P_{136}DL_{101}$	21.5	1.3	20.5	96.0

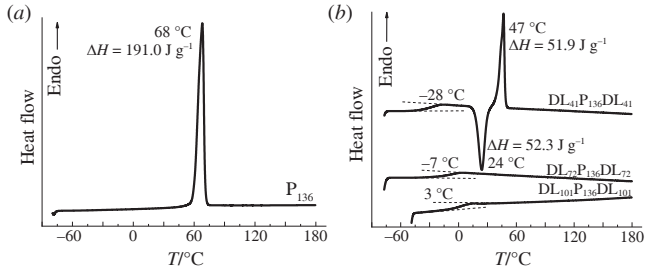

Figure 1 Second heating curves of the DSC thermograms of the samples (*a*) P_{136}; (*b*) $DL_{41}P_{136}DL_{41}$, $DL_{72}P_{136}DL_{72}$ and $DL_{101}P_{136}DL_{101}$.

The thermal behavior of the block copolymers was determined by thermogravimetric analysis (TGA) under nitrogen atmosphere, and the absence of low-molecular-weight impurities was confirmed (Figure S3, Online Supplementary Materials). The thermophysical properties of the copolymers dried for 48 h (see details in Online Supplementary Materials) were investigated by differential scanning calorimetry (DSC, see details in Online Supplementary Materials) in the temperature range from −80 to 180 °C. Figure 1 shows the DSC curves of the second heating of PEG [Figure 1(*a*)] and block copolymers [Figure 1(*b*)] after melting and cooling to −80 °C at a rate of 20 °C min^{-1}.

The heating curve of PEG [Figure 1(*a*)] contains an intense melting peak at 68 °C, in accordance with the published data.[13,14] The sample is characterized by a high degree of crystallinity (over 95%).

The DSC curve of the $DL_{41}P_{136}DL_{41}$ copolymer [Figure 1(*b*)] contains a jump corresponding to the glass transition of the hydrophilic block at −28 °C. Upon further heating, the cold crystallization of the sample occurs at 24 °C as the PEG segments become more labile, leading to crystallization. Melting of the PEG crystalline phase is observed at 47 °C, which is 20 deg lower than that of the homopolymer, as PEG is linked to the PLA blocks. However, the crystallites are not formed in hydrogel due to dissolution of the PEG block, and, consequently, do not affect the structure and the physical and mechanical properties of the material. Increasing the degree of polymerization of the hydrophobic polylactide block leads to the suppression of the PEG block crystallization even in the dry state of the copolymers $DL_{72}P_{136}DL_{72}$ and $DL_{101}P_{136}DL_{101}$ [Figure 1(*b*)].

In the investigated series of triblock copolymers, the glass transition temperature increases with increasing molecular weight and molar fraction of hydrophobic parts. All the DSC curves of block copolymer samples [Figure 1(*b*)] contain only one glass transition due to the block interaction.[15–17] Accordingly, in PLA-PEG-PLA copolymers, the PEG blocks contribute to the segmental mobility of the PLA blocks upon transition to the glassy state, which leads to the only one glass transition in the DSC thermogram.

Block copolymer hydrogel materials were prepared by the solvent replacement method (see details in Online Supplementary Materials). The as-received block copolymers were dissolved in 1,4-dioxane, being a good solvent for the both blocks, and then the organic phase was replaced by water, and aggregation of PLA blocks took place, forming a hydrogel network with PEG linking chains. It is imperative that the samples exhibit prolonged shape stability, a property that is paramount for biomedical applications.

The structure of the prepared hydrogels was studied by SAXS. The small-angle X-ray scattering curves for all polymer hydrogel samples show intense maxima in the region of scattering vectors q = 0.25–0.4 nm^{-1} [Figure 2(*a*)]. The observed peaks in the small-angle region may have a dubious origin: the scattering of an individual particle, reflecting its shape (form factor), is superimposed on Bragg diffraction maxima corresponding to the interparticle distance and the packing of higher electron density regions.[18] However, in previous works, this scattering peak is usually associated with the scattering of neighboring bridged or packed aggregates and represents the average distance between scattering centers.[18] From the q-values of the observed intense peaks, we calculated the long period [Figures 2(*a*),(*b*)], which was 17, 20, and 26 nm for $DL_{41}P_{136}DL_{41}$, $DL_{72}P_{136}DL_{72}$ and $DL_{101}P_{136}DL_{101}$, respectively.

Thus, an increase in the hydrophobic block length leads to an increase in the interplanar distances (from 17 to 26 nm), which is probably due to the formation of larger PLA aggregates in the process of polymer chain packing and the varying conformation of PEG blocks (the contour length is 38 nm).The observed differences in the supramolecular structure tend to correlate with the mechanical properties of the cross-linked systems. However, as it will be shown later, for systems with physical network junctions in the form of hydrophobic clusters, the interplanar distance does not affect directly the mechanical properties of the systems.

To evaluate the effect of the structure on the mechanical properties of hydrogels, uniaxial compression tests were performed (Figure 3). Stress–strain curves were obtained from the deformation of a series of cylindrical samples of each hydrogel (Figure S4, Online Supplementary Materials). The elastic moduli were estimated from the initial and the maximal slope of the curve.

All curves have a parabolic shape typical of cross-linked polymer systems. The elastic moduli vary nonlinearly, depending on the copolymer composition. In the case of the 1:1 block ratio, the highest value of the elastic modulus is observed, which is probably due to the optimal balance between strength and the number of nodes in the hydrogel network. In the two extreme cases in terms of composition, the elastic moduli of the materials are noticeably lower. In the case of $DL_{41}P_{136}DL_{41}$, the aggregation of shorter hydrophobic blocks leads to the formation of small aggregates. The decrease in hydrophobic interactions results in the formation of a weak physical hydrogel network. In the case of $DL_{101}P_{136}DL_{101}$, the total number of aggregates decreases significantly due to an increase in the aggregation number.

Thus, the present work demonstrates that the proposed solvent replacement method allows for the production of hydrogel materials based on P(D,L)LA-PEG-P(D,L)LA copolymers

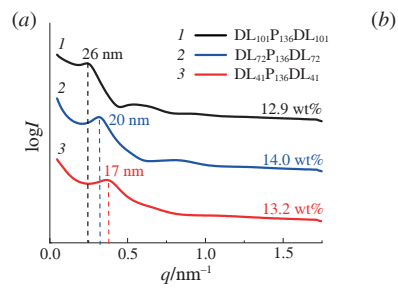

Figure 2 (*a*) Small-angle X-ray scattering curves (*d*-spacing and block copolymer mass content determined from the dry residue are indicated for each hydrogel); (*b*) schematic picture of the physical network of the hydrogel using $DL_{101}P_{136}DL_{101}$ as an example.

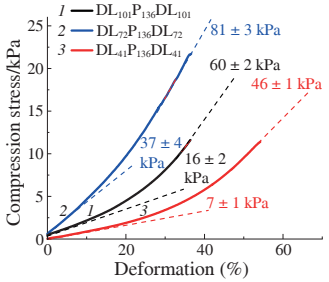

Figure 3 Compressive stress *vs.* strain curves for hydrogel samples (for each hydrogel, the initial and maximal compression moduli are shown).

with an amorphous hydrophobic block of varying composition ratios ranging from 0.6 to 1.5. The obtained hydrogel materials exhibit high elastic moduli ranging from 7 ± 1 to 37 ± 4 kPa and are capable of supporting and maintaining their shape independently, which was previously not achieved for similar systems. The characterization of the prepared hydrogels by X-ray scattering reveals the formation of ordered structures. The distance between the hard P(D,L)LA blocks serving as a network junctions depends on the molecular structure of the copolymer and changes from 17 to 26 nm with an increase in hydrophobic blocks.

Measurements of mechanical characteristics (DSC, TGA, gel permeation chromatography, and ^{1}H NMR) were carried out using the equipment of resource centers of the National Research Center 'Kurchatov Institute'. The authors are grateful to the resource centers for organic and hybrid materials 'Polymer', molecular and cell biology 'Molbiotech' of the National Research Centre 'Kurchatov Institute', as well as the Kurchatov Complex for Synchrotron and Neutron Research for providing the opportunity to perform measurements. The work was carried out within the state assignment of the NRC 'Kurchatov Institute'.

Online Supplementary Materials

Supplementary data associated with this article can be found in the online version at doi: 10.71267/mencom.7768.

References

1 S. A. Glukhova, V. S. Molchanov, Y. M. Chesnokov, B. V. Lokshin, E. P. Kharitonova and O. E. Philippova, *Carbohydr. Polym.*, 2022, **282**, 119106; https://doi.org/10.1016/j.carbpol.2022.119106.

2 E. O. Osidak, A. Y. Andreev, S. E. Avetisov, G. V. Voronin, Z. V. Surnina, A. V. Zhuravleva, T. E. Grigoriev, S. V. Krasheninnikov, K. K. Sukhinich, O. V. Zayratyants and S. P. Domogatsky, *Polymers*, 2022, **14**, 4017; https://doi.org/10.3390/polym14194017.

3 Yu. D. Zagoskin, T. E. Grigoriev, S. V. Krasheninnikov, E. V. Cuevda, E. A. Gubareva, A. V. Bakirov and S. N. Chvalun, *Dokl. Chem.*, 2019, **486**, 149; https://doi.org/10.1134/S001250081906003X.

4 X. W. Wei, Y. Ma, X. Yao, W. Zhou, X. Wang, C. Li, J. Lin, Q. He, S. Leptihn and H. Ouyang, *Bioact. Mater.*, 2021, **6**, 998; https://doi.org/10.1016/j.bioactmat.2020.09.030.

5 Y. A. Puchkova, N. G. Sedush, A. D. Ivanenko, V. G. Shuvatova, G. A. Posypanova and S. N. Chvalun, *Mendeleev Commun*., 2023, **33**, 404; https://doi.org/10.1016/j.mencom.2023.04.033.

6 Y. A. Kadina, E. V. Razuvaeva, D. R. Streltsov, N. G. Sedush, E. V. Shtykova, A. I. Kulebyakina, A. A. Puchkov, D. S. Volkov, A. A. Nazarov and S. N. Chvalun, *Molecules*, 2021, **26**, 602; https://doi.org/10.3390/molecules26030602.

7 H. Mao, P. Pan, G. Shan and Y. Bao, *J. Phys. Chem. B*, 2015, **119**, 6471; https://doi.org/10.1021/acs.jpcb.5b03610.

8 X. Yin, D. R. O. Hewitt, S. P. Quah, B. Zheng, G. S. Mattei, P. G. Khalifah, R. B. Grubbs and S. R. Bhatia, *Soft Matter*, 2018, **14**, 7255; https://doi.org/10.1039/C8SM01559G.

9 F. Yang, K. Shi, Y. Jia, Y. Hao, J. Peng, L. Yuan, Y. Chen, M. Pan and Z. Qian, *Appl. Mater. Today*, 2020, **19**, 100608; https://doi.org/10.1016/j.apmt.2020.100608.

10 F. Yang, K. Shi, Y. Hao, Y. Jia, Q. Liu, Y. Chen, M. Pan, L. Yuan, Y. Yu and Z. Qian, *Bioact. Mater.*, 2021, **6**, 3036; https://doi.org/10.1016/j.bioactmat.2021.03.003.

11 A. J. Poudel, F. He, L. Huang, L. Xiao and G. Yang, *Carbohydr. Polym.*, 2018, **194**, 69; https://doi.org/10.1016/j.carbpol.2018.04.035.

12 A. M. Desyatskova, E. V. Kuznetsova, Y. A. Puchkova, E. V. Yastremsky, A. V. Bakirov, P. V. Dmitryakov, A. I. Buzin and S. N. Chvalun, *Mendeleev Commun.*, 2023, **33**, 86; https://doi.org/10.1016/j.mencom.2023.01.027.

13 K. Pielichowski and K. Flejtuch, *Polym. Adv. Technol.*, 2002, **13**, 690; https://doi.org/10.1002/pat.276.

14 Y. Li, Q. Ma, C. Huang and G. Liu, *Mater. Sci.*, 2013, **19**, 147; https://doi.org/10.5755/j01.ms.19.2.4430.

15 Q. Wang, C. Wang, X. Du, Y. Liu and L. Ma, *J. Macromol. Sci., Part A: Pure Appl. Chem.*, 2013, **50**, 200; https://doi.org/10.1080/10601325.2013.742794.

16 K. Yasugi, Y. Nagasaki, M. Kato and K. Kataoka, *J. Controlled Release*, 1999, **62**, 89; https://doi.org/10.1016/s0168-3659(99)00028-0.

17 T. Kissel, Y. Li and F. Unger, *Adv. Drug Delivery Rev.*, 2002, **54**, 99; https://doi.org/10.1016/S0169-409X(01)00244-7.

18 S. K. Agrawal, N. Sanabria-DeLong, G. N. Tew and S. R. Bhatia, *Macromolecules*, 2008, **41**, 1774; https://doi.org/10.1021/ma070634r.

Received: 19th March 2025; Com. 25/7768